

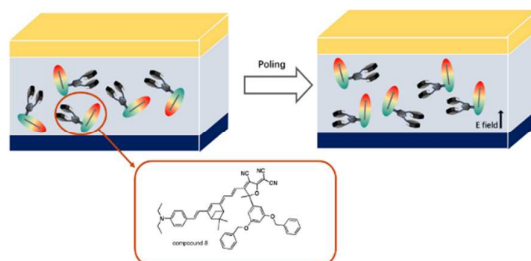


Design, Synthesis, and Properties of nonlinear optical chromophores based on verbenone bridge with novel dendritic acceptor

| | |
|-------------------------------|---|
| Journal: | <i>Journal of Materials Chemistry C</i> |
| Manuscript ID | TC-ART-01-2018-000083.R1 |
| Article Type: | Paper |
| Date Submitted by the Author: | 12-Feb-2018 |
| Complete List of Authors: | Sun, Hejing; Jilin University, The Key Laboratory for High Performance Polymer of the Ministry Education of China, College of Chemistry, Jilin University Li, Zhong'an; Huazhong University of Science and Technology, Chemistry and Chemical Engineering Wu, Jieyun; University of Electronic Science and Technology of China, Jiang, Zhenhua; Jilin University, Luo, Jingdong; University of Washington, Materials Science and Engineering Jen, Alex K-Y.; University of Washington, Materials Science and Engineering; University of Washington, Chemistry |
| | |

Table of contents entry for manuscript TC-ART-01-2018-000083
Design, synthesis, and properties of nonlinear optical chromophores based on
verbenone bridge with novel dendritic acceptor

Abstract: A polyenic chromophore containing new dendritic tricyanofuran acceptor have been synthesized for achieving improved polar order in poled polymers.





Journal Name

ARTICLE

Design, synthesis, and properties of nonlinear optical chromophores based on verbenone bridge with novel dendritic acceptor

Received 00th January 20xx,
Accepted 00th January 20xx

DOI: 10.1039/x0xx00000x

www.rsc.org/

Hejing Sun^{a,b}, Zhong'an Li^{b,c}, Jieyun Wu^{d,e}, Zhenhua Jiang^a, Jingdong Luo^{*b,d}, and Alex K.-Y. Jen^{*b,d}

Two novel second order nonlinear optical (NLO) chromophores based on N, N-diethylaniline as donors, verbenone based tetraene as bridge, and tricyanofuran (TCF) or tricyanofuran derivatives with dendritic moiety as acceptor have been synthesized in good overall yields and systematically characterized. Besides, facile applicable synthetic approach for NLO dendritic acceptor was developed. Compared with **C7**, after introducing dendritic derivative steric hindrance groups into the acceptor, chromophores **C8** had good thermal stabilities with high thermal decomposition temperatures which were 33 °C higher than chromophore **C7**. At the same time, cyclic voltammetry (CV) experiments were performed to determine the different redox properties. The conjugated verbenone tetraene segments in two chromophores could significantly improve the glass-forming ability and the molecular polarization of chromophores as revealed by UV-vis-NIR absorption measurement. The bulky dendritic moiety linked by short C-C bond is closer to the TCF acceptor, which is most polar part in the chromophore, compared to conventional isolation groups. The results obtained from electro-optic (EO) coefficients indicate that this TCF acceptor with unique dendritic structure can prevent antiparallel packing between chromophores, improving the poling efficiency and enhancing the EO performance. These properties, together with the good solubility, suggest the potential use of these new chromophores as materials for advanced photonic devices.

Introduction

Organic and polymeric second-order nonlinear optical (NLO) materials are promising enabling material systems for broadband optical modulation and terahertz photonics, due to their large electro-optic (EO) activity, relatively low dielectric constants, ultrafast response time, and exceptional processibility for large-scale integrating photonics.¹⁻⁸ In this area, one of the most critical challenges is to efficiently translate the large $\mu\beta$ values (where μ is the dipole moment, and β is the first polarizability) of the organic chromophores into high macroscopic NLO activities, since the strong intermolecular dipole-dipole interactions among the chromophore moieties in the polymeric system would impede the poling induced noncentrosymmetric alignment.⁹⁻¹²

Based on site-isolation principle, dendritic NLO materials, have been intensively explored in the NLO field, and considered to

be a very promising molecular topology for the next generation of highly efficient NLO materials, owing to their tree-like, monodisperse structures, and attractive features.¹³⁻²⁵ Since 1997, theoretical analysis and extensive experiments by Dalton and co-workers, proposed that the intermolecular electrostatic interaction could be minimized through modification of the shape of chromophores.^{3,7,14} From 2011 till now, various cross-linkable NLO dendrimers were designed, and exhibit excellent thermal stability and large optical nonlinearity, due to spatial isolation from the dendrimer shell.^{9,26,27} In 2002, taking advantage of fluorinated materials, such as high thermal stability, chemical inertness, low dielectric constants, Jen developed a novel 3-D shape chromophore shielded by highly-fluorinated dendrons, which exhibits significantly improved three times higher EO coefficient compared to its pristine analog.²⁸ They also developed a generally applicable method for the post-functionalization of side-chain dendronized NLO polymers with high poling efficiency.²⁹ In 2006, the influence of binding mode and attachment flexibility of dendritic NLO chromophores on their EO performance were investigated.³⁰ Then, inspired by arene-perfluoroarene (ArH-ArF) interaction, Jen's group developed a novel class of dendritic NLO chromophores substituted by phenyl/pentafluorophenyl dendrons which can reversibly self-assemble to build an extended supramolecular structure, in order to improve poling efficiency and good thermal stability.^{22,31} Meanwhile, they also studied the relationship between the molecular mobility energetics of

^a The Key Laboratory for High Performance Polymer of the Ministry Education of China, College of Chemistry, Jilin University, Changchun 130012, People's Republic of China.

^b Department of Materials Science and Engineering, University of Washington, Seattle, Washington 98195, USA. Email: ajen@uw.edu; Fax: +1 206 543 3100; Tel: +1 206 543 2626

^c School of Chemistry and Chemical Engineering, Huazhong University of Science & Technology, Wuhan, Hubei 430074, People's Republic of China.

^d Department of Chemistry, City University of Hong Kong, Tat Chee Avenue, Kowloon, Hong Kong SAR. Email: jingdluo@cityu.edu.hk; alexjen@cityu.edu.hk

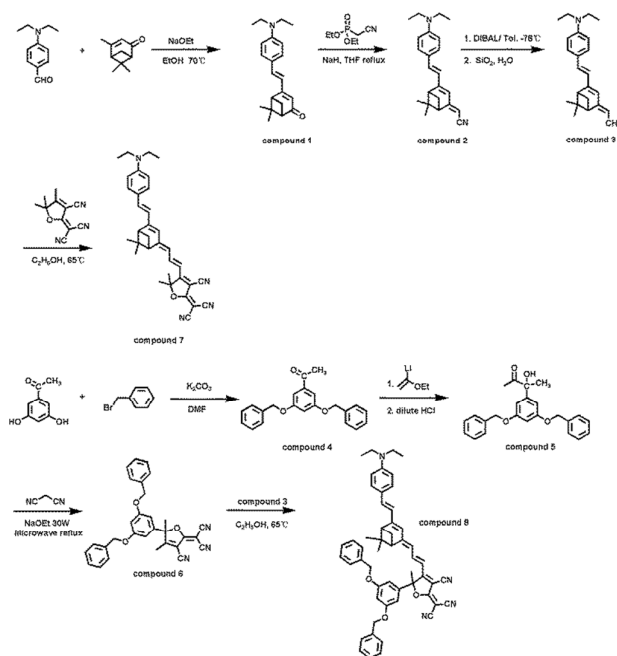
^e University of Electronic Science and Technology of China, School of Optoelectronic Science and Engineering, Chengdu 611731, People's Republic of China.

dendritic chromophores in the condensed phases and their thermal transition (relaxation) behaviour, and found that subtle variations in the dendritic molecular structure influence the critical parameters significantly.³² Recently, many novel NLO materials have employed the dendritic structures to modify NLO chromophores and polymers, and the role of the site-isolation effect in determining the material properties was systematically investigated.^{31,33-36} However, the researches of the dendritic chromophore mostly focus on modification of donor and bridge groups with flexible binding by post-modification. The dendritic acceptor, the analogue of TCF moieties, has seldom been noticed, especially for chromophores link with dendritic group by short rigid binding, possibly due to the challenge and complicated of dendritic acceptor synthesis. Most importantly, compared to electron donor and bridge, electron acceptor as most polar moiety in chromophore can have a pronounced effect on the molecular hyperpolarizability. The tricyano-dihydrofuran (TCF) acceptor, which have the unique dihydrofuran ring structure, has been increasingly used in the new generation of chromophores. The dihydrofuran ring with three cyano groups is highly planar and strongly dipolar, because of the cumulative effect of rigidly aligned cyano groups. When such acceptor is used to construct chromophores, the chromophores tends to pack antiparallel because of the strong dipole-dipole interactions. Thus, dendritic acceptor with short rigid binding is more suitable approach for preventing the chromophores from antiparallel packing and improving the poling process.³⁷⁻³⁹ This rigid short linkage makes the dendritic group closer to the acceptor than the traditional TCF acceptor, and may encapsulate the chromophore to help minimize dipole-dipole interactions and prevent aggregation. In previous research, we found that it be possible to improve material stability without increasing the cooperativity (that also means no sacrifice of efficiency) through controlling the structural rigidity of the materials.³² In this regard, we have developed a novel synthetic route to control the structural rigidity of the materials. The acceptor with dendritic moiety not only provide different dendritic structures to modify NLO chromophores, but is also expected to facilitate the preparation procedure of dendritic chromophore.

To deepen the exploration of the design parameters of novel dendritic chromophore, in this work we focus our attention on the synthesis and characterization of new chromophore **C8** with dendritic moiety on the acceptor via a rigid C-C bond, through the focused microwave assisted synthesis. Chromophore **C7** was synthesized with tricyanovinylidihydrofuran as acceptor unit for comparison. These chromophores both contain N, N-diethylaniline as donors and the same verbenone based tetraene as bridge, which has high polarization and glass-forming ability. The three-dimensional verbenone-based ring structures around the planar tetraene chain can increase steric hindrance compared to the widely used isophorone-based tetraene (CLD) bridge, and can prevent close packing of molecules and hence crystallization.⁴⁰ The solvatochromism behavior, thermal stability, electrochemical and nonlinear optical properties of

two chromophores were thoroughly investigated to understand their structure–property relationships.

Scheme 1 Chemical structures and synthetic scheme for chromophores **C7** and **C8**.



Experimental

Materials and measurements

All chemicals were purchased from Aldrich and used as received. Solvents such as tetrahydrofuran (THF), ethanol, and dibromomethane (DBM) were treated and distilled prior to use according to common purification procedures. ¹H NMR spectra were recorded on a Bruker AV300 spectrometer using CDCl₃ as solvent in all cases. High resolution mass spectrometry (HRMS) was performed on a Bruker APEX III 47e Fourier transform mass spectrometer, and ESI-MS spectra were recorded on a Bruker Daltonics Esquire ion trap mass spectrometer. Cyclic voltammetric data were measured on a BAS CV-50W voltammetric analyzer using a conventional three-electrode cell a glassy carbon working electrode, Pt wire counter-electrode, and Ag/AgCl reference electrode at a scan rate of 100 mVs⁻¹. The 0.1 M tetrabutyl ammonium hexafluorophosphate (TBAPF) in CH₂Cl₂ is the electrolyte. UV-vis-NIR spectra were recorded on a UV Varian Cary 5000 UV-Vis-NIR Spectrophotometer. Microwave irradiations were carried out on a CEM Discovery focused microwave system. Thermogravimetric analysis(TGA) were performed on a Pyris 1 thermogravimetric analyzer.

Poling and r₃₃ measurements

For studying the EO property derived from the chromophores, guest–host polymers were generated by formulating chromophores **C7** and **C8** into poly(methyl methacrylate) (PMMA) using DBM as the solvent. The resulting solutions were filtered through a 0.2 μm PTFE filter and spin-coated

onto thin-film device (TFD) indium tin oxide (ITO) glass substrates. Films of doped polymers were baked in a vacuum oven at 60 ° C overnight to ensure the removal of the residual solvent. Then, a thin layer of gold was sputtered onto the films as a top electrode for contact poling. The r_{33} values were measured using the Teng–Man simple reflection technique at the wavelength of 1310nm.

Compound 1. To a solution of 4-(diethylamino)benzaldehyde (2.00 g, 11.28 mmol) and (1S)-(-)-verbenone (2.04 g, 13.58 mmol) in anhydrous ethanol was added a freshly prepared solution of sodium ethoxide (14.35 mmol) by syringe. The reaction mixture was stirred at 70 ° C for 24 h and then was poured into a saturated solution of ammonium chloride and extracted with ethyl acetate; the combined organic extracts were washed with brine and dried over Na_2SO_4 . After removal of the solvent, the residue was purified by column chromatography using hexane/ ethyl acetate as eluent to give the product as red solids (2.66 g, yield: 76%). $^1\text{H NMR}$ (CDCl_3 , 300 MHz, ppm): δ 7.40 (d, J = 7.8 Hz, 2H,Ar-H), 6.83 (dd, J = 36.6, 16.0 Hz, 2H, CH), 6.66 (d, J = 7.8 Hz, 2H Ar-H), 5.85 (s, 1H ,CH), 3.42 (d, J = 6.5 Hz, 4H, NCH_2), 3.15 (s, 1H,CH), 2.91 (d, J = 4.4 Hz, 1H, CH_2), 2.72 (s, 1H,CH), 2.13 (d, J = 9.2 Hz, 1H, CH_2), 1.59 (s, 3H, CH_3), 1.20 (t, J = 13.8 Hz, 6H, CH_3), 1.04 (s, 3H, CH_3). MS: calcd for $\text{C}_{21}\text{H}_{27}\text{NO}$:309.2 ; found : 310.1

Compound 2. Under N_2 atmosphere to the mixture of NaH (0.133 g, 5.54 mmol) in dry THF was added diethyl cyanomethylphosphonate (0.98 g, 5.52 mmol) dropwise by syringe at 0 ° C with an ice bath. After the solution became clear, compound 1 (0.85 g, 2.75 mmol) in dry THF was added. The mixture was refluxed for 3 h and then poured into a saturated solution of ammonium chloride and extracted with ethyl acetate; the combined organic extracts were washed with brine and dried over Na_2SO_4 . After removal of the solvent, the residue was purified by column chromatography using hexane/ethyl acetate as eluent to give the product as orange-red solids (0.78 g, yield: 85%). The ratio of the Z : E isomers is 60 : 40% calculated by the integration of respective protons. $^1\text{H NMR}$ (CDCl_3 , 300 MHz, ppm): δ 7.35 (s, 2H,Ar-H), δ 6.74 (s, 1H,CH), 6.66 (d, J = 8.0 Hz, 2H,Ar-H), 6.50 (s, 0.6H,CH), 6.07 (s, 0.4H,CH), 4.94 (s, 0.4H,CH), 4.82 (s, 0.6H,CH), 3.41 (d, J = 5.9 Hz, 4H,N CH_2), 3.01 (s, 1H,CH), 2.72 (s, 2H, CH_2), 1.54 (d, J = 15.4 Hz, 3H, CH_3), 1.25 (d, J = 22.6 Hz, 6H, CH_3), 0.87 (s, 3H, CH_3). MS: calcd for $\text{C}_{23}\text{H}_{28}\text{N}_2$ 332.48 ; found : 333.1

Compound 3. The solution of compound 2 (0.5 g, 1.50 mmol) in dry toluene was cooled to -78 ° C and the solution of diisobutyl aluminum hydride (DIBAL) in hexane (1.0 M, 2.6 mL, 2.6 mmol) was added dropwise by syringe. After being kept at -78 ° C for 2 h, wet silica gel was added to quench the reaction and the mixture was stirred at 0 ° C for 2 h. The product mixture was filtered off, and the resulting precipitates were washed with ethyl acetate. Evaporation of the solvent and purification by column chromatography using hexane/ethyl acetate as eluent gave the product as dark red oil (0.39 g, yield: 78%). The ratio of the Z : E isomers is 40 : 60%

calculated by the integration of respective protons. $^1\text{H NMR}$ (300 MHz, CDCl_3) δ 10.14 (d, J = 8.2 Hz, 0.4H,CHO), 9.89 (d, J = 8.5 Hz, 0.6H, CHO), 7.44 – 7.27 (m, 2.4H,Ar-H), 6.93 (s, 0.6H,CH), 6.71 (t, J = 9.6 Hz, 2.4H,Ar-H), 6.63 (d, J = 8.7 Hz, 2H, CH), 6.09 (s, 1H,CH), 5.84 (d, J = 8.5 Hz, 0.6H,CH), 5.62 (d, J = 8.1 Hz, 0.4H,CH), 3.39 (dd, J = 14.0, 7.0 Hz, 4H,N CH_2), 3.03 (d, J = 4.9 Hz, 1H,CH), 2.87 – 2.57 (m, 1H,CH), 1.89 – 1.66 (m, 2H, CH_2), 1.66 – 1.45 (m, 5H, CH_3), 1.20 (dd, J = 17.9, 11.0 Hz, 6H, CH_3), 0.89 (d, J = 1.7 Hz, 4H, CH_3). MS: calcd for $\text{C}_{23}\text{H}_{29}\text{NO}$ 335.5; found : 336.2

Compound 4. A mixture of benzyl bromide (4.47 g, 26.3 mmol), 3,5-dihydroxyacetophenone (2.0 g, 13.15 mmol), potassium carbonate (3.63 g, 26.3 mmol), and KI(0.33g,1.97mmol) was dissolved in dry DMF. The reaction mixture was heated at 85 ° C for 20 h. After cooling to room temperature, the reaction mixture was poured into water. The mixture was extracted with CH_2Cl_2 and dried. After removal of the solvents under reduced pressure, the residue was purified by column chromatography to give a white solid product. (3.49g, yield: 80%) $^1\text{H NMR}$ (300 MHz, CDCl_3) δ 7.59 – 7.28 (m, 10H, Ar-H), 7.20 (s, 2H,Ar-H), 6.81 (d, J = 1.4 Hz, 1H,Ar-H), 5.07 (s, 4H, CH_2), 2.56 (s, 3H, CH_3). HRMS(ESI) (M^+ , $\text{C}_{22}\text{H}_{20}\text{O}_3$): calcd:332.1412; found: 333.1499

Compound 5. To a solution of ethyl vinyl ether (15mmol,1.08g) in THF was added 5.9ml of t-BuLi(1.7M,10mmol) in pentane dropwise at -78 ° C, under nitrogen for 2h. To a solution was warmed on ice bath and stirred for 1h. And then cooled to -78 ° C. A solution of compound 4 (5mmol, 1.66g) in THF was added the lithiated ether solution dropwise at -78 ° C. The resulting mixture was stirred for 1h at -78 ° C, allowed to warm up to room temperature slowly for 2h. The reaction was then quenched with 30ml of NH_4Cl aqueous, and the mixture was extracted with CH_2Cl_2 . The combined organic layer was washed with water and dried with magnesium sulfated. After the solvent was evaporated, the residue is dissolved in 20ml methanol and added dropwise HCl(aq) (1M, 6mmol) at room temperature. The exothermal reaction was cooled using a water bath and monitored by thin layer chromatography(TLC). After stirring for 2h, the resulting mixture was neutralized with NaHCO_3 , concentrated via rotary evaporation, and extracted with CH_2Cl_2 . After the solvent was evaporated, the product was purified by chromatography to give a white solid (1.22 g, yield: 65%). $^1\text{H NMR}$ (CDCl_3 , 300 MHz, ppm): δ 7.52 – 7.30 (m, 10H, Ar-H), 6.67 (s, 2H, Ar-H), 6.57 (s, 1H, Ar-H), 5.18 – 4.92 (m, 4H, CH_2), 4.56 (s, 1H,OH), 2.00 (d, J = 34.0 Hz, 3H, CH_3), 1.73 (s, 3H, CH_3) HRMS(ESI) (M^+ , $\text{C}_{24}\text{H}_{24}\text{O}_4$):calcd: 376.1675 ; found: 377.1714

Compound 6. Compound 5(1mmol, 376mg), malonitrile (2 mmol, 132mg) and NaOEt (0.15mmol) in ethanol was heated under 30W microwave reflux for 30 min. Solvent was removed by rotary evaporation and residue was purified via flash chromatography on silica gel with a gradient eluent of CH_2Cl_2 to 2% EtOH in CH_2Cl_2 to afford solid product. (293 mg, yield: 62%). $^1\text{H NMR}$ (CDCl_3 , 300 MHz, ppm): δ 7.40 (d, J = 3.3 Hz, 10H,Ar-H), 6.65 (d, J = 13.3 Hz, 1H, Ar-H), 6.31 (d, J = 2.1 Hz, 2H,Ar-H), 5.04 (d, J = 7.9 Hz, 4H, CH_2), 2.22 –

1.98 (m, 3H, CH₃), 1.87 (d, J = 17.3 Hz, 3H, CH₃). HRMS(ESI) (M⁺, C₃₀H₂₃N₃O₃):calcd: 473.1739; found: 474.1835

Compound 7. Compound 3 (101 mg, 0.3 mmol) and TCF acceptor (59 mg, 0.3 mmol) were dissolved in the mixture solvent of anhydrous ethanol and CH₂Cl₂. The reaction mixture was allowed to stir at 65 °C for 4 h and monitored by TLC. After removal of the solvents, the residue was purified by column chromatography eluting with hexane/ethyl acetate. Further purification of the product by reprecipitation from methanol/ dichloromethane afforded the desired chromophore as dark solids (124mg, yield: 80 %). The ratio of the Z: E isomers is 30: 70% calculated by the integration of respective protons. ¹H NMR (CDCl₃, 300 MHz, ppm): δ 8.27 (t, J = 13.4 Hz, 0.3H,CH), 8.02 (t, J = 13.7 Hz, 0.7H,CH), 7.40 (d, J = 7.9 Hz, 2H,Ar-H), 7.29 (s, 3H), 6.92 – 6.73 (m, 2H,CH), 6.72 – 6.56 (m, 2H,Ar-H), 6.22 (dd, J = 27.8, 16.5 Hz, 2H,CH), 6.04 (d, J = 12.8 Hz, 0.3H,CH), 3.43 (d, J = 6.7 Hz, 4H, CH₂), 3.30 (s, 0.7H,CH), 3.13 (s, 1.3H,CH), 2.82 (d, J = 20.7 Hz, 1.7H, CH₂), 1.79 (d, J = 8.9 Hz, 1.3H, CH₃), 1.69 (d, J = 12.8 Hz, 6H, CH₃), 1.59 (d, J = 11.3 Hz, 6H, CH₃), 1.22 (t, J = 6.7 Hz, 6H, CH₃), 0.88 (s, 3H, CH₃). HRMS(ESI) (M⁺, C₃₄H₃₆N₄O):calcd: 516.2889; found: 517.2975

Compound 8. Compound 3 (101 mg, 0.3 mmol) and compound 6 (142mg, 0.3 mmol) were dissolved in the mixture solvent of anhydrous ethanol and CH₂Cl₂. The reaction mixture was allowed to stir at 65 °C for 12 h and monitored by TLC. After removal of the solvents, the residue was purified by column chromatography eluting with hexane/ethyl acetate. Further purification of the product by reprecipitation from methanol/ dichloromethane afforded the desired chromophore as dark solids (137mg, yield: 58%). The ratio of the Z: E isomers is 20: 80% calculated by the integration of respective protons. ¹H NMR (CDCl₃, 300 MHz, ppm): δ 7.91(m,0.2H,CH),7.73(m,0.3H,CH),7.48 – 7.27 (m, 12H,Ar-H), 6.85 – 6.70 (m, 1H,Ar-H), 6.63 (d, J = 8.7 Hz, 2H,Ar-H), 6.55 (d, J = 8.7 Hz, 0.5H,Ar-H), 6.49 (s, 1H,CH), 6.45 (s, 1H,CH), 6.32 (d, J = 8.1 Hz, 1H,Ar-H), 6.13 (t, J = 13.9 Hz, 2H,CH), 5.87 (d, J = 12.2 Hz, 0.5H,CH), 5.05 (d, J = 9.9 Hz, 4H, CH₂), 3.40 (d, J = 6.7 Hz, 4H, CH₂), 3.05 (s, 1H,CH), 2.89 (s, 0.3H, CH₂), 2.70 (s, 1H,CH), 2.10 (s, 0.3H, CH₂), 2.04 – 1.82 (m, 3H, CH₃), 1.68 (d, J = 9.1 Hz, 1H, CH₂), 1.53 (d, J = 10.6 Hz, 4H, CH₃), 1.45 (s, 2H, CH₃), 1.21 (dd, J = 16.6, 9.8 Hz, 6H, CH₃), 0.81 (d, J = 6.5 Hz, 2H, CH₃), 0.67 (s, 1H, CH₃). HRMS(ESI) (M⁺, C₅₃H₅₀N₄O₃):calcd: 790.3883; found: 791.3973

Results and discussion

Synthesis and characterization of chromophores

Scheme 1 shows the chemical structures and synthetic approach for this series of ring-locked tetraene chromophores **C7** and **C8**. These chromophores were designed to have the same electron donor N, N-diethylaniline group and the (1S)-(-)-verbenone-based tetraene bridge, but to have the different side groups on the acceptor. The novel functional acceptor with Fréchet-type benzyl ether dendrons of generations of 1

was synthesized in three steps. The precursor dendritic ketones were prepared according to the literature.^{41,42} Then, ethyl vinyl ether was reacted with t-butyllithium at -78 ° C and the vinyl anion formed. The dendritic ketones were added to the vinyl lithium solution, with the anion reacting with the prochiral ketone. After acid hydrolysis, the racemic α-ketol was obtained as shown in Scheme 1. Through the focused microwave assisted synthesis,⁴³ the α-ketol with dendritic substituent is condensed with malononitrile under basic conditions to form the 2,5-dihydrofuran-derived electron acceptor(C6). Starting from amine donor, N-ethyl-N-(2-hydroxyethyl) aminobenzaldehyde, the novel verbenone based bridge was synthesized in good overall yields through simple 3-step reactions. In the presence of sodium ethoxide as the base, (1S)-(-)-verbenone reacted directly with amine donor via the Knoevenagel condensation to obtain the corresponding aminophenyldienone derivatives. The extension of the conjugated π-bridge to yield the key aminophenyltrienal intermediates was accomplished in good overall yields by condensing the dienones with diethyl(cyanomethyl)phosphonate using the Wittig–Horner reaction, followed by reducing the resultant trienenitriles with DIBAL and subsequent hydrolysis. Finally, the novel acceptor with dendritic substituent and a TCF type acceptor were condensed with verbenone-based tetraene bridge to afford the desired phenyltetraene-based chromophores **C8** and **C7**, respectively. All these chromophores possess good solubility in common organic solvents, such as dichloromethane, THF and acetone. All the chromophores were completely characterized by ¹H NMR, MS, UV-Vis spectroscopic analysis and the data obtained were in full agreement with the proposed formulations.

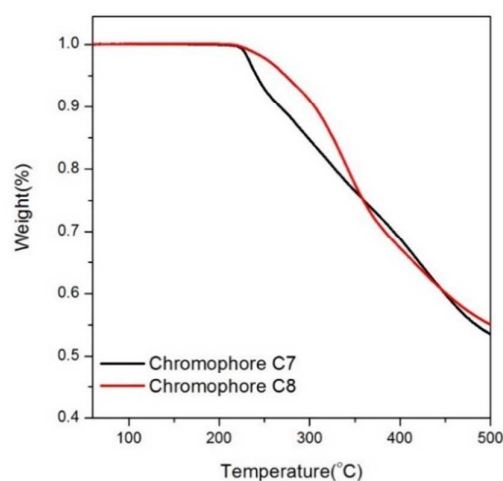


Fig. 1 TGA curves of chromophores **C7** and **C8** with a heating rate of 10°C min⁻¹ in a nitrogen atmosphere.

Thermal stability

The NLO chromophores must be thermally stable in order to withstand the poling process and subsequent processing for

use. To investigate the thermal stability of the chromophore, thermogravimetric analysis (TGA) was used with a heating rate of $10\text{ }^{\circ}\text{C min}^{-1}$ under nitrogen atmosphere. TGA curve of the chromophores is shown in Fig. 1. The two chromophores with a similar verbenone structure on the π -electron bridge exhibited good thermal stabilities with the decomposition temperatures (T_d) higher than $220\text{ }^{\circ}\text{C}$. The chromophore **C8** had the highest decomposition temperature ($T_d = 273\text{ }^{\circ}\text{C}$), followed by **C7** ($T_d = 240\text{ }^{\circ}\text{C}$). While chromophore **C8** had a much higher decomposition temperature than chromophore **C7** with no steric hindrance on the acceptor. The enhanced thermal stability of chromophores **C8** over chromophore **C7** is due to the introduction of dendric group derivative steric hindrance groups into acceptor. These data indicate that the novel TCF acceptor with dendric steric hindrance groups can help to increase the thermal stability of the chromophore. The excellent thermal stability of these chromophores makes them suitable for practical device fabrication and EO device preparation.

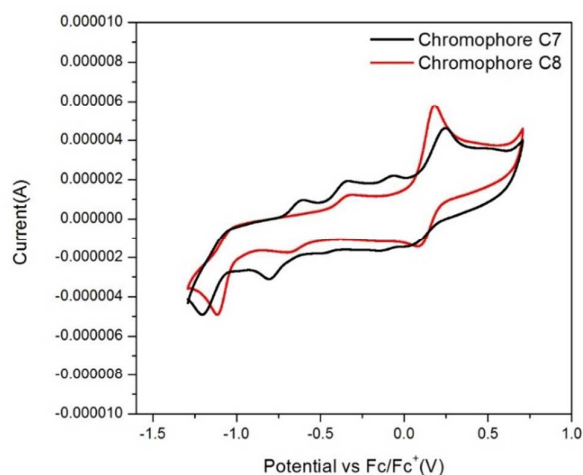


Fig. 2 Cyclic voltammograms of chromophores **C7** and **C8** recorded in CH_2Cl_2 solutions containing a 0.1 M TBAPF supporting electrolyte at a scan rate of 100 mV s^{-1} .

Electrochemical properties

To determine the redox properties of chromophores, cyclic voltammetry (CV) measurements were conducted in degassed anhydrous dichloromethane solutions containing 0.1 M tetrabutylammonium hexafluorophosphate (TBAPF) as the supporting electrolyte. The relative data and voltammograms of $1 \times 10^{-4}\text{ mol L}^{-1}$ chromophores **C7** and **C8** were recorded. As shown in Fig. 2, chromophores **C7** and **C8** both exhibited one quasi reversible oxidative wave with a half-wave potential, $E_{1/2} = 0.5(E_{\text{ox}} + E_{\text{red}})$, versus ferrocene/ferrocenium at about 0.142 , 0.14 V respectively. Meanwhile, these chromophores had an irreversible reduction wave corresponding to the acceptor

moieties at $E_{\text{red}} = -1.213\text{ V}$ and -1.114 V . This may suggest that the strength of the electron acceptor could be increased by replacing the methyl group with the dendritic moiety substituent. This may result from the fact that dendritic moiety has a stronger electron-withdrawing ability than methyl group. The energy gaps between the HOMO and LUMO energy for chromophores **C7** and **C8** were 1.382 eV and 1.364 eV , respectively, while the chromophore FTC exhibited the energy gap (DE) values of 1.529 eV .³⁰ This comparison demonstrated that the new verbenone based bridge narrowed the energy gap indicating the excellent charge-transfer of verbenone based bridge chromophore.

The HOMO and LUMO levels of two chromophores were calculated from their corresponding oxidation and reduction potentials. The HOMO levels of **C7** and **C8** were estimated to be -4.89 eV and -4.85 eV , respectively. And, the corresponding LUMO level of **C7** and **C8** were estimated to be -3.51 eV , -3.49 eV , respectively.

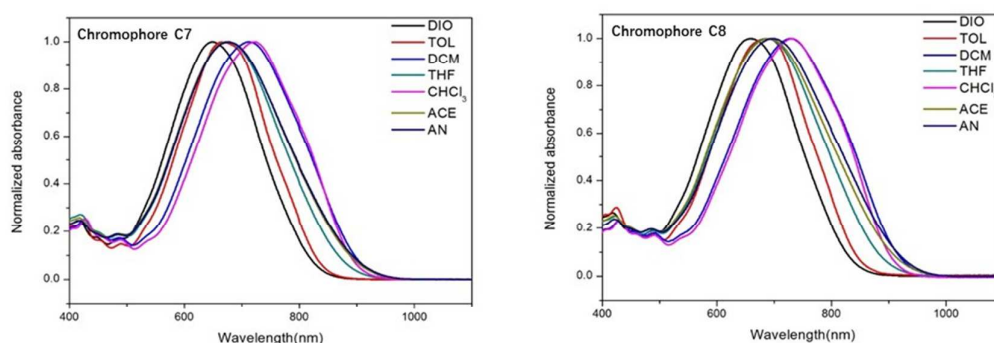
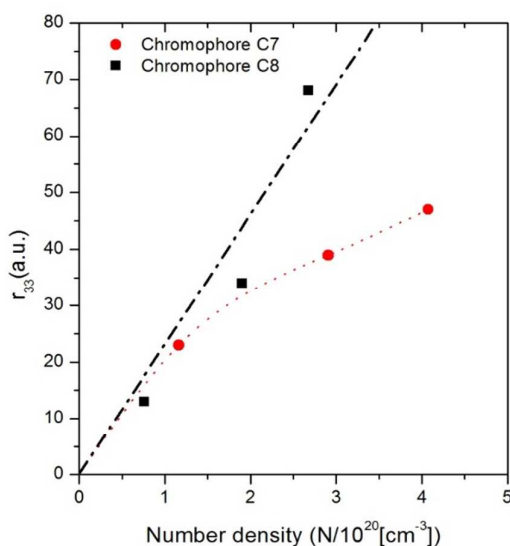
Optical properties

To explore the different charge-transfer (CT) absorption properties of each chromophore, UV-Vis absorption spectra of two chromophores were measured in series solvents with different dielectric constants. As shown in Fig. 3, chromophores **C7** and **C8** exhibited the maximum absorption (λ_{max}) at 723 nm and 731 nm in chloroform, respectively. Compared to chromophore **C7**, chromophore **C8** showed blue shifted ($\Delta=8\text{ nm}$), it attributes to the different acceptors: the dendritic group would enhance the electron-withdrawing ability of acceptor. It may somehow enhance the strength of the acceptor. The spectrum data are summarized in Table 1. Besides, the solvatochromic behavior was also an important aspect to investigate the polarity of chromophores. When increasing the solvent dielectric constant, all of the two chromophores showed very large bathochromic shifts of 74 nm and 72 nm from dioxane to chloroform, respectively. **C7** and **C8** display larger solvatochromism than that of CLD (60 nm)⁴⁴ and a FTC (61 nm)⁴⁵ chromophore. It indicated that all chromophores **C7** and **C8** are more polarizable than the traditional chromophore CLD and FTC. With a further increase of solvent polarity, saturation behavior was found for both chromophores in more polar solvents, such as acetone, and acetonitrile. For example, **C7** and **C8** showed hypsochromic shifts of 45 nm and 41 nm , respectively, from chloroform to acetone. Such a phenomenon was reported by Davies⁴⁶ and was ascribed to the back-electron transfer from the acceptor side to the donor side in polar solvents which causing blue-shift from the absorption⁴⁷.

Table 1 Spectral data and the absorption maxima of the chromophores **C7** and **C8** in seven kinds of solvents with varying dielectric constant

| Compd | Absorption Maximum (nm) | | | | | | | $\Delta\lambda^a$ |
|-----------|-------------------------|---------|-----------------|-----------------|------------|---------|--------------|-------------------|
| | Dioxane | Toluene | Dichloromethane | Tetrahydrofuran | Chloroform | Acetone | Acetonitrile | |
| C7 | 649 | 671 | 714 | 673 | 723 | 678 | 678 | 74 |
| C8 | 659 | 685 | 729 | 689 | 731 | 690 | 699 | 72 |

$$^a \Delta\lambda = \lambda_{\max}(\text{chloroform}) - \lambda_{\max}(\text{dioxane})$$

**Fig. 3** UV-Vis absorption spectra of chromophores **C7** and **C8** in seven kinds of aprotic solvents with varying dielectric constants.**Fig. 4** Comparison of the EO coefficients of NLO chromophores **C7** and **C8** containing different loading densities and substituent modifications.

Electro-optic performance

To testify the effect of novel dendritic acceptor on the EO activities, the r_{33} values of films **C7**/PMMA and **C8**/PMMA were measured in different loading densities, as shown in Fig. 4. **C7** and **C8** displayed excellent compatibility with the polymer matrix when guest-host polymers were prepared. For chromophore **C7**, the r_{33} values gradually improved from 23 pm V^{-1} (10 wt%) to 47 pm V^{-1} (35 wt%). However, as shown in Table 2, N-normalized r_{33} (r_{33}/N), which effectively normalizes the r_{33} value for the relative chromophore content, decrease with the increasing number density. This can be explained by the fact that, when in a low-density range, the intermolecular dipolar interactions are relatively weak, the performance of the materials was more related to the intrinsic molecular properties. With the increasing of the chromophore density, the intermolecular dipole-dipole interactions would become stronger and stronger, and leads to the unfavorable antiparallel packing of chromophores. It could not translate the microscopic hyperpolarizability into macroscopic EO response effectively. The graph becomes nonlinear.

Films of **C8** were prepared at 10, 25, and 35 total chromophore wt %, corresponding to 0.762 , 1.905 , and 2.677×10^{20} molecules/cc, respectively. When the concentration of the

chromophore in PMMA is low, film **C7**/PMMA displayed a larger r_{33} value than that of film **C8**/PMMA. As the chromophore loading increased, this trend is reversed. Meanwhile, compare to **C7**, N-normalized r_{33} (r_{33}/N) of **C8** maintain high values and were not decreased with increasing of chromophore content. Fig. 5 shows schematic illustration for chromophore **C8** poling processes. At the close chromophore number (N) density (25wt% for **C7** and 35wt% for **C8**), the contribution of every chromophore to the r_{33} value (r_{33}/N) of **C8** (25.40) is nearly two times of **C7** (13.40). And as the chromophore loading density increase, the r_{33}/N of **C8** increased, rather than decrease for **C7**. Due to optimized configurations of **C8** that the rigid C-C bond linked dendritic moiety on the acceptor encapsulate the chromophores effectively to prevent forming the antiparallel dimer, and

provide more space for efficient orientation of the chromophores, it could help to keep chromophore-chromophore electrostatic interactions to a low level, and improve the poling process. It means this unique dendritic structure might be desirable in reducing dipole-dipole interactions and prevailing parallel pattern, resulting in translating the microscopic hyperpolarizability into macroscopic EO response more effectively. Besides, solvatochromic behavior indicated that chromophores **C7** and **C8** are more easily polarizable than chromophore CLD and FTC. Therefore, in poling process, chromophores **C7** and **C8** may obtain orientation more easily in contrast with chromophore CLD and FTC.

Table 2 Physical properties and EO coefficients of chromophores **C7** and **C8**.

| Compounds | Wt% | r_{33} (pm/V) ^a | N ^b | r_{33}/N ^c |
|-----------|-----|------------------------------|----------------|-------------------------|
| C7 | 10 | 23 | 1.164 | 19.75 |
| | 25 | 39 | 2.911 | 13.40 |
| | 35 | 47 | 4.075 | 11.53 |
| C8 | 10 | 13 | 0.762 | 17.06 |
| | 25 | 34 | 1.905 | 17.84 |
| | 35 | 68 | 2.677 | 25.40 |

^aExperimental value from simple reflection at 1310 nm. ^b Chromophore number density; in units of $\times 10^{20}$ molecules/cc. ^c r_{33} normalized by chromophore number density; in units of $\times 10^{20}$ pm cc/(V molecules).

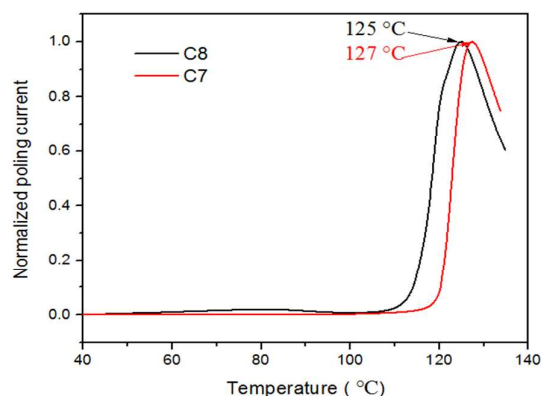


Fig. 5 The normalized poling current of chromophore alignment as a function of temperature in PMMA.

In terms of temporal stability of electro-optic coefficients, widely adaptable strategies include the self-assembled dendrimers, simple guest-host doping with high glass transition temperature. For **C7** and **C8** in host PMMA with the relatively close chromophore number density (25wt% for **C7** and 35wt% for **C8**), despite of the different molecular structures, their films showed very similar highest poling temperatures, which are dictated by their glass transition

temperatures during poling, respectively (shown in Fig. 5). In such typical guest-host systems with PMMA as the host, their temporal stability of electro-optic coefficients at room temperature is around 90% after initial fast decay and then tend to be stabilized. Such temporal stability is routine and it indicated that their stability is related to the glass transition temperature. We expect good temporal stability at the elevated temperatures can be achievable by using polymers with the higher glass transition temperature, which will be reported in due course.

Hence, the electro-optic activities showed that dendritic chromophore **C8** showed a higher poling efficiency comparing to **C7**. It indicated that introduction of dendrimer in the acceptor can effectively attenuate the chromophore static dipole-dipole interactions (Fig. 6).

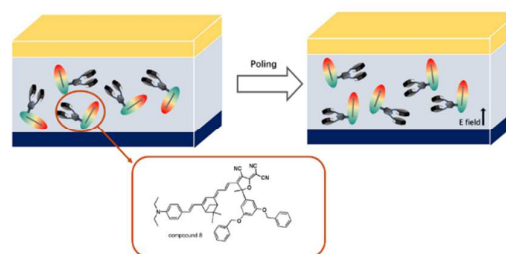


Fig. 6 Proposed scheme of poling processes to generate the macroscopic polar order of chromophore **C8** in polymer matrix.

Conclusions

In this article, two NLO chromophores **C7** and **C8** based on N, N-diethylaniline as donors and tricyanovinylidihydrofuran (TCF) acceptors (**C7**) or tricyanovinylidihydrofuran (TCF) acceptors with dendritic moiety (**C8**) linked together via verbenone based tetraene π -conjugation as the bridges have been synthesized and systematically characterized by NMR, MS and UV-Vis absorption spectroscopy. Thermogravimetric analysis showed that chromophore **C8** had excellent thermal stability with a decomposition temperature of 273 °C, and this decomposition temperature was 33 °C higher after introducing the dendritic substituent steric hindrance group into the acceptor when compared with chromophore **C7**. The effects of bathochromic and solvatochromic behavior on the UV-Vis absorption were also investigated to compare different electron withdrawing abilities and polarizabilities. Both two chromophores showed good solubility and comparability with the polymer which were crucial for making high quality EO devices. Incorporation of chromophores **C7** and **C8** into PMMA provided large electro-optic coefficients of 47 and 68 pm V⁻¹ at 1310 nm with a high loading of 35 wt%. Moreover, dendritic substituent can reduce dipole-dipole interactions for high efficient poling at high chromophore loading density. The number of aligned chromophores (translated microscopic hyperpolarizability into macroscopic electro-optic coefficients) was nearly two times of **C7**. It also suggests intelligently designed dendritic EO chromophores as promising candidates for further development.

Conflicts of interest

There are no conflicts to declare.

Acknowledgements

This work was supported by Air Force Office of Scientific Research (FA8650-14-C-5005), New Faculty Start-up Grant of City University of Hong Kong (7200550), and the State-Sponsored Scholarship for Graduate Students from China Scholarship Council.

Notes and References

- J. Luo, S. Huang, Z. Shi, B. M. Polishak, X.-H. Zhou and A. K.-Y. Jen, *Chem. Mater.*, 2011, **23**, 544-553.
- H. Ma, A. K.-Y. Jen, J. Wu, X. Wu and S. Liu, *Chem. Mater.*, 1999, **11**, 2218-2225.
- S. R. Marder, *Chem. Commun.*, 2006, **37**, 131-134.
- D. R. Kanis, M. A. Ratner and T. J. Marks, *Chem. Rev.*, 1994, **94**, 195-242.
- J. H. Wülbern, S. Prorok, J. Hampe, A. Petrov, M. Eich, J. Luo, A. K.-Y. Jen, M. Jenett and A. Jacob, *Optics Letters*, 2010, **35**, 2753-2755.
- S. R. Marder, B. Kippelen, A. K.-Y. Jen and N. Peyghambarian, *Nature*, 1997, **388**, 845.
- Y. Shi, C. Zhang, H. Zhang, J. H. Bechtel, L. R. Dalton, B. H. Robinson and W. H. Steier, *Science*, 2000, **288**, 119-122.

- M. Lee, H. E. Katz, C. Erben, D. M. Gill, P. Gopalan, J. D. Heber and D. J. McGee, *Science*, 2002, **298**, 1401-1403.
- Z. Shi, J. Luo, S. Huang, X.-H. Zhou, T.-D. Kim, Y.-J. Cheng, B. M. Polishak, T. R. Younkin, B. A. Block and A. K.-Y. Jen, *Chem. Mater.*, 2008, **20**, 6372-6377.
- J. Wu, C. Peng, H. Xiao, S. Bo, L. Qiu, Z. Zhen, and X. Liu, *Dyes and Pigments*, 2014, **104**, 15-23.
- C. Hu, F. Liu, H. Zhang, F. Huo, Y. Yang, H. Wang, H. Xiao, Z. Chen, J. Liu, L. Qiu, Z. Zhen, X. Liu and S. Bo, *J. Mater. Chem. C*, 2015, **3**, 11595-11604.
- C. Hu, Z. Chen, H. Xiao, Z. Zhen, X. Liu and S. Bo, *J. Mater. Chem. C*, 2017, **5**, 5111-5118.
- H. Zhang, H. Xiao, F. Liu, F. Huo, Y. He, Z. Chen, X. Liu, S. Bo, L. Qiu and Z. Zhen, *J. Mater. Chem. C*, 2017, **5**, 1675-1684.
- W. Wu, C. Ye, J. Qin and Z. Li, *ACS Appl. Mater. Interfaces*, 2013, **5**, 7033-7041.
- M. Li, Y. Li, H. Zhang, S. Wang, Y. Ao and Z. Cui, *J. Mater. Chem. C*, 2017, **5**, 4111-4122.
- L. R. Dalton, S. J. Benight, L. E. Johnson, D. B. Knorr, I. Kosilkin, B. E. Eichinger, B. H. Robinson, A. K.-Y. Jen and R. M. Overney, *Chem. Mater.*, 2011, **23**, 430-445.
- T. Gray, T.-D. Kim, D. B. Knorr, J. Luo, A. K.-Y. Jen and R. M. Overney, *Nano Lett.*, 2008, **8**, 754-759.
- H. Ma, A. K.-Y. Jen and L. R. Dalton, *Adv. Mater.*, 2002, **14**, 1339-1365.
- S. Hecht and J. M. J. Fréchet, *Angew. Chem. Int. Ed.*, 2001, **40**, 74-91.
- S. M. Grayson and J. M. J. Fréchet, *Chem. Rev.*, 2001, **101**, 3819-3867.
- J. Wu, H. Xiao, L. Qiu, Z. Zhen, X. Liu, and S. Bo, *Rsc Advances*, 2014, **4**, 49737-49744.
- T.-D. Kim, J.-W. Kang, J. Luo, S.-H. Jang, J.-W. Ka, N. Tucker, J. B. Benedict, L. R. Dalton, T. Gray, R. M. Overney, D. H. Park, W. N. Herman and A. K.-Y. Jen, *J. Am. Chem. Soc.*, 2007, **129**, 488-489.
- S.-H. Jang and A. K.-Y. Jen, *Chem. Asian J.*, 2009, **4**, 20-31.
- H. Ma, S. Liu, J. Luo, S. Suresh, L. Liu, S. H. Kang, M. Haller, T. Sassa, L. R. Dalton and A. K.-Y. Jen, *Adv. Funct. Mater.*, 2002, **12**, 565-574.
- T.-D. Kim, J. Luo, Y.-J. Cheng, Z. Shi, S. Hau, S.-H. Jang, X. H. Zhou, Y. Tian, B. Polishak, S. Huang, H. Ma, L. R. Dalton and A. K.-Y. Jen, *J. Phys. Chem. C*, 2008, **112**, 8091-8098.
- H. Ma, B. Chen, T. Sassa, L. R. Dalton and A. K.-Y. Jen, *J. Am. Chem. Soc.*, 2001, **123**, 986-987.
- J. Luo, M. Haller, H. Ma, S. Liu, T.-D. Kim, Y. Tian, B. Chen, S.-H. Jang, L. R. Dalton and A. K.-Y. Jen, *J. Phys. Chem. B*, 2004, **108**, 8523-8530.
- J. Luo, H. Ma, M. Haller, A. K.-Y. Jen and R. R. Barto, *Chem. Commun.*, 2002, **8**, 888-889.
- J. Luo, S. Liu, M. Haller, L. Liu, H. Ma and A. K.-Y. Jen, *Adv. Mater.*, 2002, **14**, 1763-1768.
- P. A. Sullivan, A. J. P. Akelaitis, S. K. Lee, G. McGrew, S. K. Lee, D. H. Choi and L. R. Dalton, *Chem. Mater.*, 2006, **18**, 344-351.
- X.-H. Zhou, J. Luo, S. Huang, T.-D. Kim, Z. Shi, Y.-J. Cheng, S.-H. Jang, D. B. Knorr, R. M. Overney and A. K. Y. Jen, *Adv. Mater.*, 2009, **21**, 1976-1981.
- D. B. Knorr, X.-H. Zhou, Z. Shi, J. Luo, S.-H. Jang, A. K.-Y. Jen and R. M. Overney, *J. Phys. Chem. B*, 2009, **113**, 14180-14188.
- P. A. Sullivan, H. Rommel, Y. Liao, B. C. Olbricht, A. J. P. Akelaitis, K. A. Firestone, J.-W. Kang, J. Luo, J. A. Davies, D. H. Choi, B. E. Eichinger, P. J. Reid, A. Chen, A. K.-Y. Jen, B. H. Robinson and L. R. Dalton, *J. Am. Chem. Soc.*, 2007, **129**, 7523-7530.
- S. R. Hammond, J. Sinness, S. Dubbury, K. A. Firestone, J. B. Benedict, Z. Wawrzak, O. Clot, P. J. Reid and L. R. Dalton, *J. Mater. Chem.*, 2012, **22**, 6752-6764.

Journal Name

ARTICLE

- 35 J. Luo, M. Haller, H. Li, H.-Z. Tang and A. K.-Y. Jen, *Macromolecules*, 2004, **37**, 248-250.
- 36 M. Faccini, M. Balakrishnan, M. B. J. Diemeer, Z.-P. Hu, K. Clays, I. Asselberghs, A. Leinse, A. Driessen, D. N. Reinhoudt and W. Verboom, *J. Mater. Chem.*, 2008, **18**, 2141-2149.
- 37 Y. Liao, B. E. Eichinger, K. A. Firestone, M. Haller, J. Luo, W. Kaminsky, J. B. Benedict, P. J. Reid, A. K.-Y. Jen, L. R. Dalton and B. H. Robinson, *J. Am. Chem. Soc.*, 2005, **127**, 2758.
- 38 T. L. Kinnibrugh, T. V. Timofeeva, O. Clot, A. Akelaitis and L. R. Dalton, *Acta Crystallogr., Sect. E*, 2006, **62**, o4804.
- 39 S. Li, M. Li, J. Qin, M. Tong, X. Chen, T. Liu, Y. Fu, S. Wu and Z. Su, *CrystEngComm*, 2009, **11**, 589-596.
- 40 X.-H. Zhou, J. Davies, S. Huang, J. Luo, Z. Shi, B. Polishak, Y.-J. Cheng, T.-D. Kim, L. Johnson and A. K.-Y. Jen, *J. Mater. Chem.*, 2011, **21**, 4437-4444.
- 41 J. Zou, B. Guan, X. Liao, M. Jiang and F. Tao, *Macromolecules*, 2009, **42**, 7465-7473.
- 42 C. J. Hawker and J. M. J. Fréchet, *J. Am. Chem. Soc.*, 1990, **112**, 7638-7647.
- 43 S. Liu, M. A. Haller, H. Ma, L. R. Dalton, S.-H. Jang and A. K.-Y. Jen, *Adv. Mater.*, 2003, **15**, 603-607.
- 44 C. Zhang, L. R. Dalton, M. C. Oh, H. Zhang and W. H. Steier, *Chem. Mater.*, 2001, **13**, 3043-3050.
- 45 X. Piao, X. Zhang, S. Inoue, S. Yokoyama, I. Aoki, H. Miki, A. Otomo and H. Tazawa, *Org. Electron.*, 2011, **12**, 1093-1097.
- 46 J. A. Davies, A. Elangovan, P. A. Sullivan, B. C. Olbricht, D. H. Bale and T. R. Ewy, C. M. Isborn, B. E. Eichinger, B. H. Robinson, P. J. Reid, X. Li and L. R. Dalton, *J. Am. Chem. Soc.*, 2008, **130**, 10565-10575.
- 47 X. Ma, F. Ma, Z. Zhao, N. Song and J. Zhang, *J. Mater. Chem.*, 2010, **20**, 2369-2380.